J. Inst. Electrostat. Jpn.

静電気学会誌, **28**, 5 (2004) 265-271

論　　文

Electrohydrodynamic Flow Patterns in a Nozzle-Plate Electrostatic Precipitator

Marek KOCIK[*,1], Jarosław DEKOWSKI[*], Jerzy MIZERACZYK[*], Jen-Shih CHANG[**], Seiji KANAZAWA[***] and Toshikazu OHKUBO[***]

(Received September 11, 2003; Accepted July 13, 2004)

In this paper results of the Particle Image Velocimetry (PIV) measurements of the flow velocity fields in a nozzle-plate type electrostatic precipitator (ESP) are presented. The presented results confirmed a strong interaction of the electric field, electric charge and the main flow, resulting in the downstream and upstream vortex-type flow patterns due to electrohydrodynamic (EHD) secondary flow (of a velocity of several tens of cm/s). This investigation shows that when the nozzle discharge electrode is used, the vortexes generated by the EHD forces revolve in the opposite direction to the vortexes generated in ESPs with the smooth wire discharge electrode. The flow structures for the nozzle electrode are more stable than those for the smooth wire electrode.

1. Introduction

In recent years a special environmental concern is directed towards controlling the emission of micron and submicron particles in ESPs, which operating with high overall efficiency, are not effective in the removal of fine particles (size range from 0.1 to 1 μm). Many of the fine particles of the size of 1 μm and less contain toxic trace elements. Hence, there has long been an interest in improving ESP collection of fine particles.

The motion and precipitation of particles in the duct of an ESP depend on the particle properties, electric field, space charge and gas flow. It was shown[1-7] that a significant interaction between these factors exists, resulting in considerable unsteady turbulent flow patterns in the ESP. The numerical results of the particle collection efficiency[8] showed that the fine particle collection could be significantly improved if the electric wind were eliminated. However, there is a lack of experimental evidences whether the electric wind advances or deteriorates fine particle precipitation process. To elucidate the influence of the electrically generated flow disturbances on the precipitation of fine particles in ESPs more experimental investigations are needed.

In this paper results of the PIV measurements of the flow velocity fields in a nozzle-plate type ESP are presented. The nozzles-plate is a representative electrode geometry not only for ESPs with barbed wire but also for corona radical shower[9].

The presented experiment is a part of larger work which focuses on the mapping of the flow patterns for different ESPs geometries and working parameters (e.g., main gas flow velocity, discharge current). This can be helpful for elucidating the motion and precipitation of the particles (in particular 0.1 to 1 μm).

Key words: electrostatic precipitator, electrohydrodynamic (EHD) flow, PIV, submicron particle precipitation

* Centre for Plasma and Laser Engineering, Institute of Fluid Flow Machinery, Polish Academy of Sciences, Fiszera 14, 80-231 Gdańsk, Poland

** Department of Engineering Physics, McMaster University Hamilton, Ontario, L8S 4M1 Canada

*** Department of Electrical and Electronic Engineering, Oita University, 700 Dannoharu, Oita 870-1192, Japan

[1] kocik@imp.gda.pl

2. Experimental set-up

The apparatus used in this experiment consisted of an ESP and a standard PIV equipment for the measurement of flow velocity field (Fig.1).

The ESP was made of an acrylic box (100 mm x 200 mm x 1000 mm). A stainless-steel pipe (4 mm in diameter) with nozzles was used as the discharge nozzle electrode.

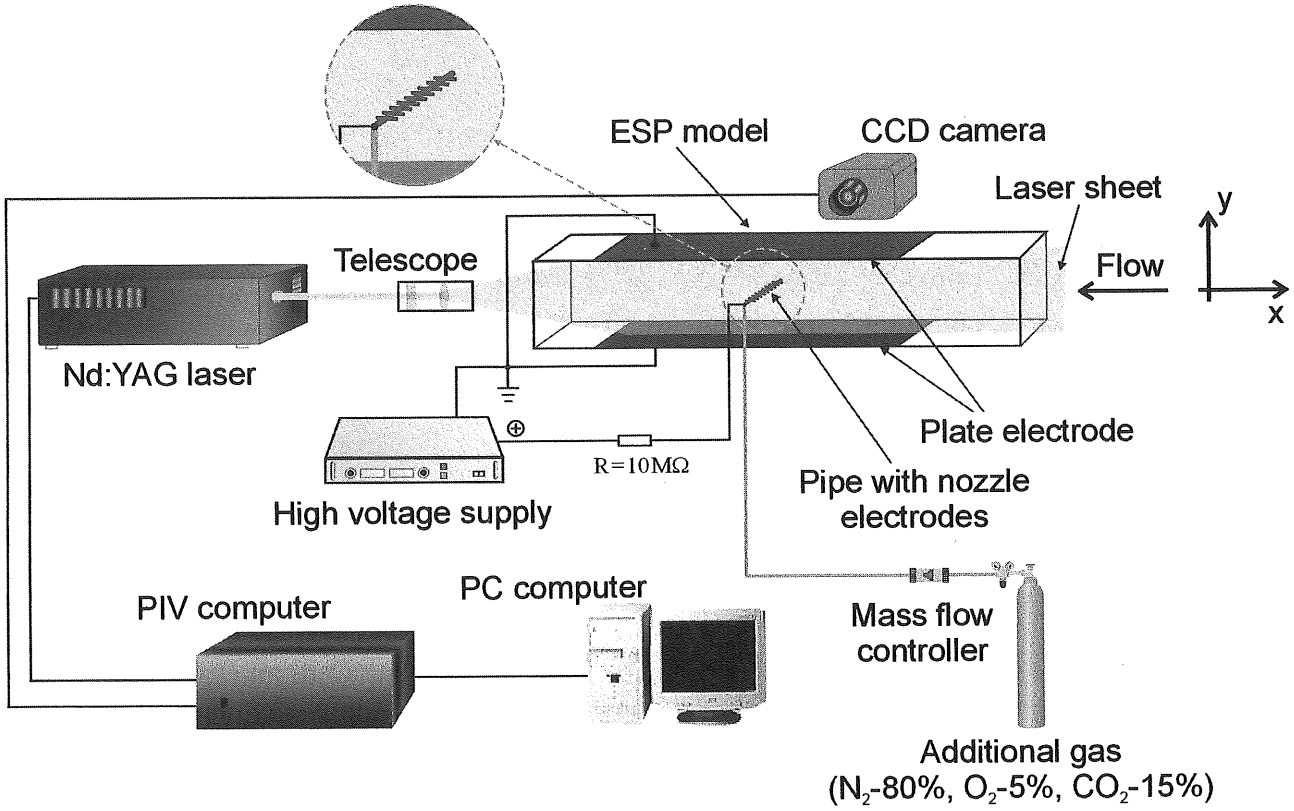

Fig. 1. Experimental set-up.

It was mounted in the middle of the ESP, in the halfway between two grounded parallel plate electrodes (200 mm x 600 mm), as shown in Fig. 1. 18 nozzle electrodes (1.5 mm outer diameter, 1 mm inner diameter, 5 mm length, 20 mm apart from each other) was soldered into the pipe. Positive polarity DC high voltage was applied through a 10 MΩ resistor to the pipe. The operating voltage was set around 31 kV to develop a stable streamer corona discharge from each nozzle to the plate electrodes. The total time-averaged discharge current was about 150 μA.

Two gas flow, the main and the additional, were established in the ESP. The main gas flow (ambient air) was generated by a fan. The average velocity of the main gas flow was varied from 0 to 0.6 m/s, which is typical of the flow in ESPs. The standard deviation of the mean main gas flow velocity was ± 4 %. The main gas flow was seeded with cigarette smoke (particle size of less than 1 μm in dry air) for the PIV measurements (for laser light scattering). The additional gas (N_2:O_2:CO_2=80%:5%:15%) was injected through the nozzles into the main gas flow with a flow rate 0.5 L/min (averaged velocity at the nozzle was 0.6 m/s). The presence of CO_2 (15 %) stabilized the streamer corona discharge mode, preventing the glow corona made and the transition to the spark discharge mode.

The discharge electrode arrangement used in this investigation resembles a barbed wire electrode used in ESPs and a nozzle electrode in the so-called corona radical shower reactors[9], in which an additional flow through the nozzles is used.

The PIV equipment was the same as used by Mizeraczyk et al[10]. The laser sheet, which formed the observation plane, passed through the central nozzle, perpendicularly to the plate electrodes.

We assumed that the flow in the ESP is symmetric with respect to the horizontal plane (parallel to the plate electrodes) passing through the discharge electrode. Therefore, the measurement area (monitored by the CCD camera) was limited to the lower half of the ESP.

The velocity field maps presented in this paper are composed of several adjacent velocity fields (from 2 to 4 fields), each of an area of 75 mm x 75 mm. All the presented velocity field maps resulted from the averaging of 100 measurements, i.e. the presented velocity maps are time-averaged.

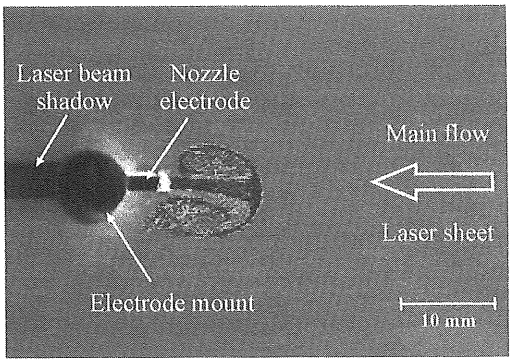

Fig. 2. Image (side view) of the additional flow structure for an additional gas flow rate of 0.5 L/min. The averaged main gas flow velocity of 0.2 m/s. No voltage applied. The main gas was ambient air seeded with cigarette smoke, and the additional gas was unseeded ambient air.

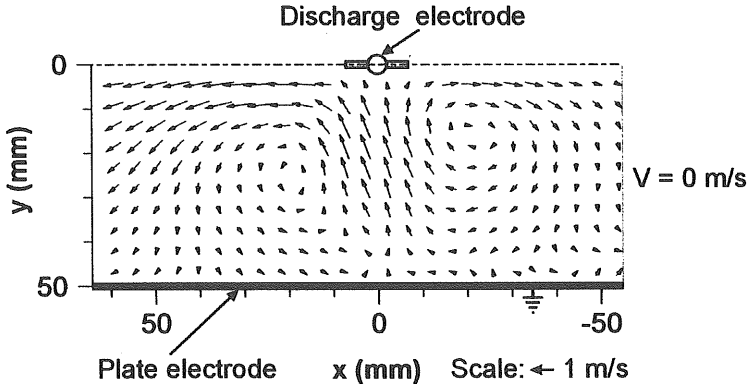

Fig. 3. Time-averaged flow velocity field in the ESP without a main gas flow (the observation plane through the central nozzle). Positive voltage polarity, time-averaged discharge current 150 μA, additional gas flow rate 0.5 L/min.

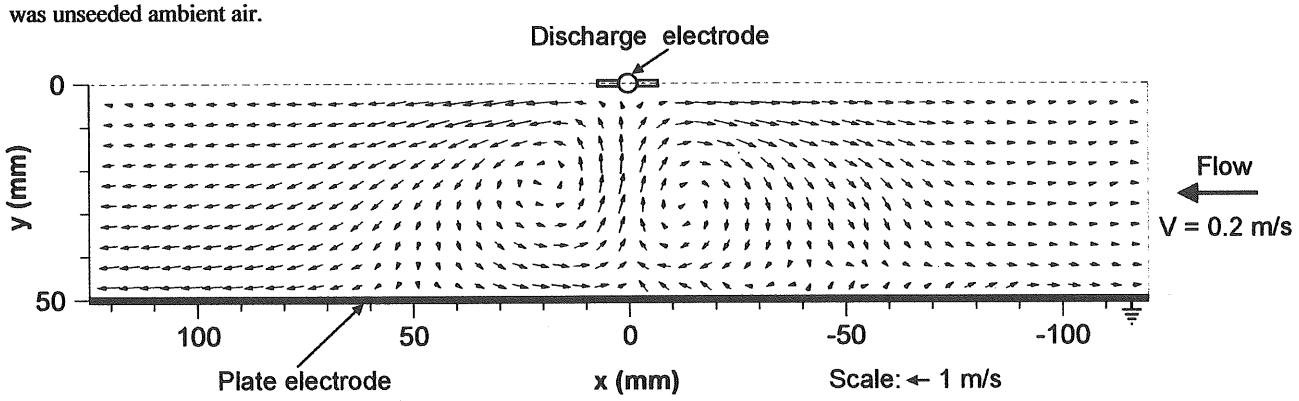

was unseeded ambient air.

Fig. 4. Time-averaged flow velocity field in the ESP at a main gas flow velocity of 0.2 m/s (the observation plane through the central nozzle). Positive voltage polarity, time-averaged discharge current 150 μA, additional gas flow rate 0.5 L/min.

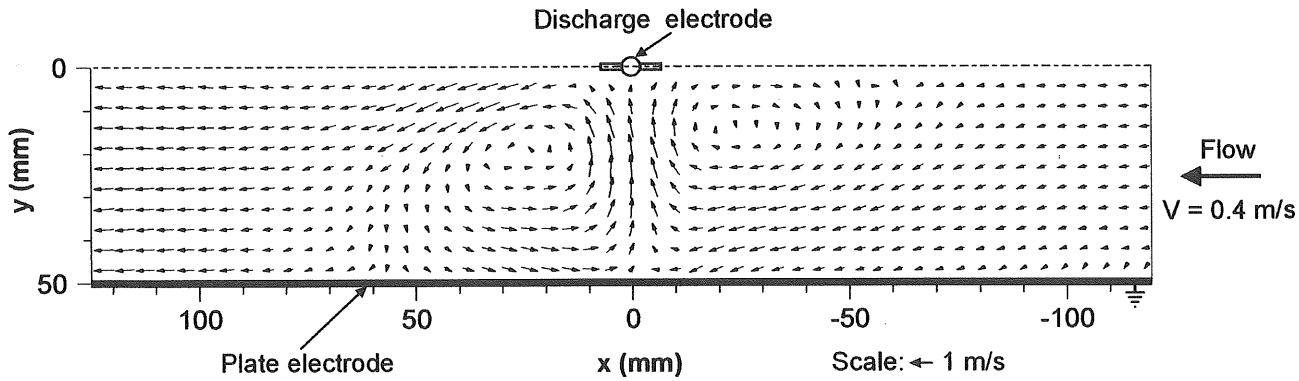

Fig. 5. Time-averaged flow velocity field in the ESP at a main gas flow velocity of 0.4 m/s (the observation plane through the central nozzle). Positive voltage polarity, time-averaged discharge current 150 μA, additional gas flow rate 0.5 L/min.

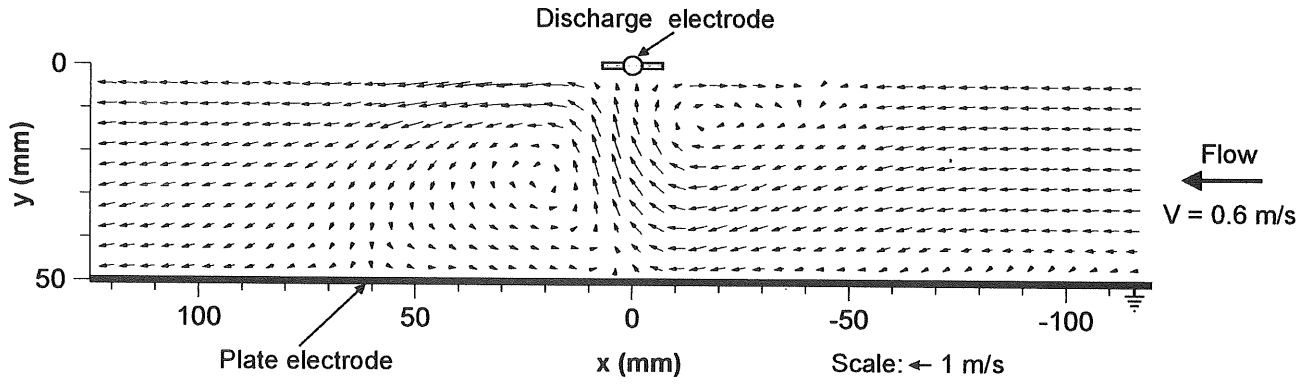

Fig. 6. Time-averaged flow velocity field in the ESP at a main gas flow velocity of 0.6 m/s (the observation plane through the central nozzle). Positive voltage polarity, time-averaged discharge current 150 μA, additional gas flow rate 0.5 L/min.

The electrohydrodynamic number E_{hd} used in this paper is expressed by the equation:

$$E_{hd} = \frac{I_s L_s^3}{\rho \nu^2 \mu_i A},$$

where: I_s is the total current, L_s is the distance between the discharge and plate electrodes, ρ is the gas density, ν is the gas dynamic viscosity, μ_i is the ion mobility, A is the electrode surface area (the area of both plates participating in the discharge).

3. Results

The corona discharge source was the edge of each nozzle, and there was no discharge from either the nozzle pipes nor the supporting pipe. The results on the current density distribution for the nozzle-plate geometry were presented in[11].

Fig. 2 shows a blow-up image of the electrically undisturbed additional gas flow (no applied voltage) at the upstream side of the nozzle when the main gas velocity was relatively low (V= 0.2 m/s). It is seen from Fig. 2 that the additional gas flow influenced the main gas flow only in a small region due to the massive countercurrent flow of the main gas. At higher main gas flow velocities, this influence was smaller. When an EHD force existed in the flow, both flow, the main gas and additional gas flow were influenced by the EHD force. As we observed (not photographed), the additional gas flow was considerably suppressed by the EHD force. Due to it the influence of the additional gas flow on the main gas flow became even smaller.

The flow velocity field patterns in the ESP for four different time-averaged velocities of the main gas flow (0, 0.2, 0.4 and 0.6 m/s) at a constant discharge current of about 150 μA, additional gas flow rate of 0.5 L/min are shown in Figs. 3 - 6. The schematic streamlines of the flow are shown in Fig. 7. Due to the significant EHD flow, all the observed flow patterns were unsteady. Therefore all the images presented in Figs. 3 - 7 were time-averaged over 1 min.

The results of the PIV measurements presented in Figs. 3 - 7 show strong EHD secondary flow in the ESP. As seen from the presented results, the EHD secondary flow patterns depend on velocity of the main gas flow.

The direction of rotation of the electrohydrodynamically caused vortexes is opposite to that observed in the ESP with the smooth wire discharge electrode[10]. As seen in Figs. 3 - 7, in the case of the nozzle electrode, the flow in the upstream and downstream vortexes near the nozzle electrode move from the nozzle first against (upstream vortex) or along (downstream vortex) the main gas flow, then turn towards the plate electrodes, and eventually return to the discharge electrode. This is in contrary to the rotation of the vortexes when the smooth wire electrode is used, where the flow vortexes begin their motion from the smooth wire electrode directly towards the plate electrodes, and then they turn to return to the wire electrode. Thus, the near discharge electrode vortexes revolve in the opposite direction to those for the nozzle electrode case studied in this work.

Without the main gas flow, strong vortexes are formed at both sides of the discharge electrode (Figs. 3 and 7). The velocity of the additional gas flowing out of the nozzles is about 0.6 m/s (measured by the PIV and calculated from the flow rate). Reynolds number of the nozzle jet (calculated using the outer diameter of the nozzle) is about $Re_{(n)}$ = 59 and the electrohydrodynamic number for the nozzle outlet is $E_{hd(n)}$ = 2 x

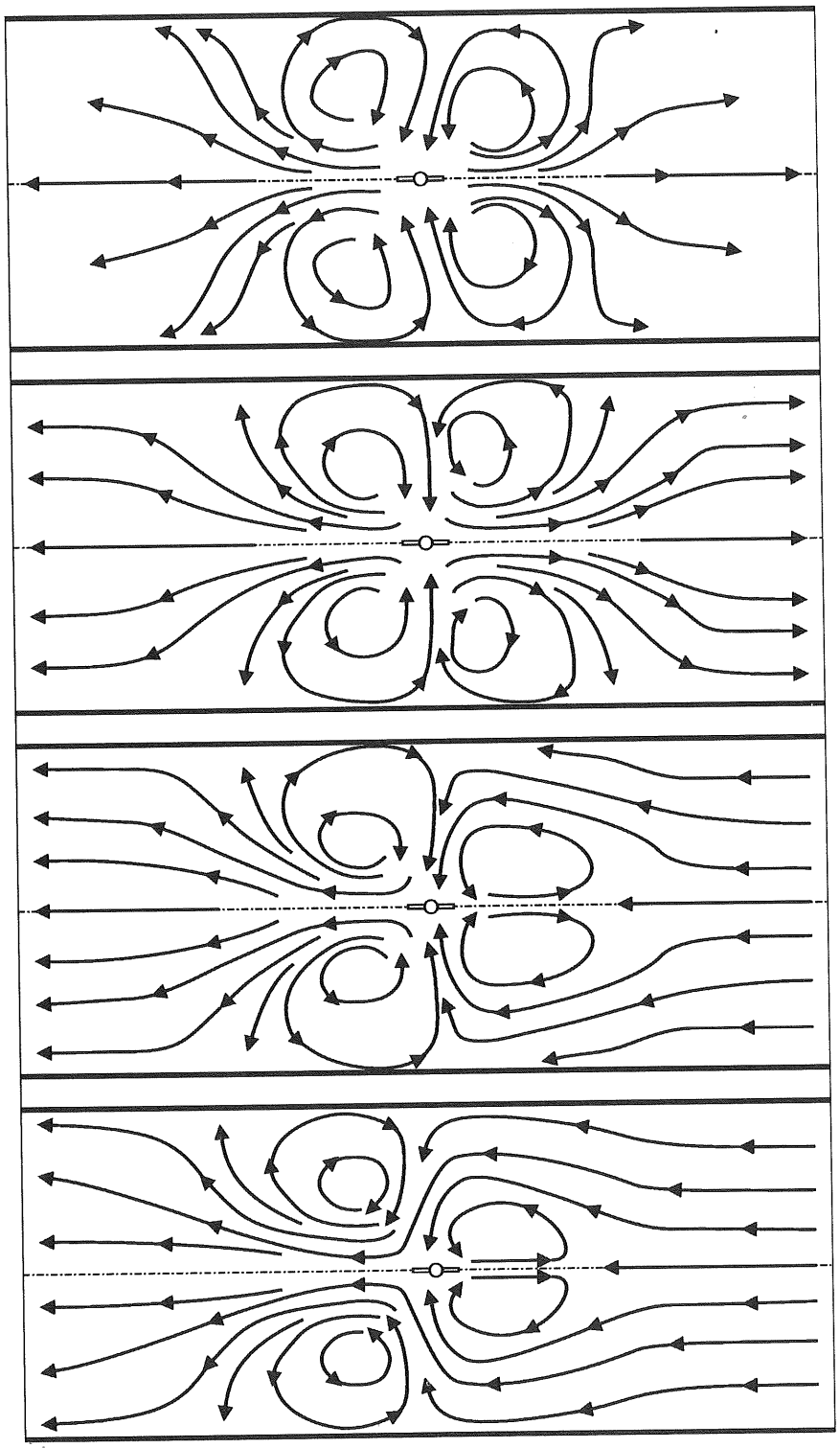

Fig. 7. Schematic streamlines of the flow in the ESP at different main gas flow velocities (0, 0.2, 0.4, 0.6 m/s). The observation plane through the central nozzle, positive voltage polarity, time-averaged discharge current 150 μA, additional gas flow rate0.5 L /min. The ratio $E_{hd(m)}/Re_{(m)}^2$ is calculated for the whole duct.

10^5 [12,13] (subscript n stands for "nozzle"). Therefore, the flow around the nozzle, apparent as the strong vortexes, seems to be dominated by the electrohydrodynamic forces (the ratio of the EHD number to Reynolds number squared $E_{hd(n)}/Re_{(n)}^2 = 58$). The following reasoning explains the minor role of the additional gas flow in the near-nozzle vortex forming. As mentioned, the averaged flow velocity of the upstream additional gas flow is 0.6 m/s, while the averaged main gas flow velocities are from 0.2 m/s to 0.6 m/s. Hence, a large main gas flow (from 216L/min to 960L/min) suppresses easily the additional gas jet from the electrode nozzles (0.5L/min) and quenches it in the vicinity of the nozzle. As a result, the countercurrent flow jet extinguishes at a distance of 1.5 cm from the nozzle when the main gas flow velocity is 0.2 m/s, as shown in Fig. 2 (see also Mizeraczyk et al.[14]). Due to the co-current jet of the downstream additional gas flow, the flow pattern in the downstream region is different from that in the upstream region, as seen in Fig. 3. However, this co-current additional gas flow does not generate any vortex because $Re_{(n)}^2 << E_{hd(n)}$, as discussed.

At a relatively low main flow velocity of 0.2 m/s (Reynolds number for the duct, based on the distance between discharge and plate electrodes, is $Re_{(m)} = 1326$, m – stands for "main gas flow"), also strong vortexes are formed in both the upstream and downstream region around the discharge electrode (Figs. 4 and 7). However, the upstream vortexes become to be shrunk by the main gas flow. At the main gas flow velocity of 0.2 m/s, the electric force is still dominating over the inertial one (the E_{hd} number for the region of 10 cm around the discharge electrode is $E_{hd(m)} = 46.4 \times 10^6$, while the ratio $E_{hd(m)}/Re_{(m)}^2 = 26.4$). At the main gas flow velocity of 0.2 m/s the flow does not pass through discharge zone in the plane consisting the nozzle (Figs. 4 and 7). This indicates that there must exist a flow transverse to that plane, which means that the flow is three-dimensional, as earlier predicted for other ESP geometries in[6,7].

The relatively better in its symmetry flow pattern at V = 0.2 m/s compared to that at V = 0 m/s is seemed to be a result of the time-averaging of the unsteady flow, or of the nonlinear EHD effect. Both possible causes need future investigations.

The increase in the main gas flow velocity to 0.4 – 0.6 m/s diminishes the influence of the electric forces on the gas flow. Figs. 5, 6 and 7 show that the vortexes at the upstream side of the discharge electrode become smaller. The main gas flow, still influenced by the EHD secondary flow, first passes between upstream vortexes and the electrode plates, then it turns towards the discharge electrode, and eventually it moves between both downstream vortexes along the middle of the duct. At a main gas flow velocity of 0.4 m/s ($Re_{(m)} = 2650$, $E_{hd(m)}/Re_{(m)}^2 = 6.6$) the upstream vortexes shrink only slightly (Figs. 5 and 7), but at V = 0.6 m/s ($Re_{(m)} = 3974$, $E_{hd(m)}/Re_{(m)}^2 = 3$), the upstream vortexes become about 3 times smaller than the downstream vortexes (Figs. 6 and 7).

4. Conclusions

The presented results of the PIV measurements of the flow velocity fields are representative for the ESP with barbed wire or corona radical shower electrodes.

The results showed that the role of the additional gas flow is negligible compared with the main gas flow under the present operating conditions. The results confirmed the existence of a strong interaction between the electric field, electric charge and the main gas flow, which resulted in the vortex-type flow patterns due to the EHD secondary flow (the electric wind). The electric wind has velocity of several tens of cm/s. Because of the strong electric wind we can expect that the fine particle collection will be poor[8].

It was found in this investigation that when the barbed wire discharge electrode is used, the vortexes generated by the EHD forces revolve in the opposite direction to the vortexes generated in ESPs with smooth wire discharge electrodes. The flow structures in the ESP with the barbed wire electrode are more stable than those for the ESPs with smooth wire electrodes[10].

The flow patterns presented in this paper concerned the cross-section passing through the central nozzle of the discharge electrode (2-D measurement). However, they suggest that the electric wind in our ESP is a three-dimensional phenomenon, similarly as in other ESP geometries[6,7]. Consequently, the measurements of the flow patterns in the cross-sections between the electrode nozzles and in horizontal cross-sections are under way to reveal 3-D flow patterns in our ESP.

Acknowledgments

This work was supported by the Foundation for Polish Science (Fundacja na Rzecz Nauki Polskiej, subsidy 8/2001),

the State Committee for Scientific Research (grant KBN PB 1756/T10/01/21) , the Institute of Fluid Flow Machinery, Polish Academy of Sciences, Gdańsk (grant IMP PAN O3/Z-3/T2), and the Canadian-Japanese-Polish Scientific Cooperation.

References

1) T. Ohkubo, Y. Nomoto, T. Adachi, and K. J. McLean: J. Electrostat., **18** (1986) 289
2) P. Atten, F. M. J. McCluskey and A. C. Lahjomri: IEEE Trans. Ind. Appl., **23-4** (1987) 705
3) C. L. Chang and H. Bai: Aerosol Sci. Techn., **33-3** (2000) 228
4) A. Mizuno: IEEE Trans. Dielectr. Electric. Insul., **7-5** (2000) 615
5) T. Yamamoto, M. Okuda, and M. Okubo: Proceedings of 2002 IEJ Annual Meeting (Toyahashi), (2002) 105
6) T. Yamamoto, H. R. Velkoff: J. Fluid Mech., **108** (1981) 1
7) T. Yamamoto, M. Okuda, and M. Okubo: IEEE Trans. Ind. Appl., **39** (2003) 1602
8) U. Kogelschatz, W. Egli and E.A. Gerteisen, ABB Review, **4** (1999) 33
9) T. Ohkubo, S. Kanazawa, Y. Nomoto, J.S. Chang, and T. Adachi: IEEE Trans. Ind. Appl., **30** (1994) 856
10) J. Mizeraczyk, M. Kocik, J. Dekowski, M. Dors, J. Podliński, T. Ohkubo, S. Kanazawa, and T. Kawasaki: J. Electrostat., **51-52** (2001) 272
11) S. Shimamoto, S. Kanazawa, T. Ohkubo, Y. Nomoto, J. Mizeraczyk, J. S. Chang: J. Electrostat., **61** (2004) 223
12) IEEE-DEIS-EHD Technical Committee: IEEE Trans. Dielectr. Electric. Insul., **10-1** (2003) 3
13) J.S. Chang and A. Watson, IEEE Trans. Dielectr. Electric. Insul., **1** (1994) 871-895
14) J. Mizeraczyk, J. Podliński, M. Dors, M. Kocik, T. Ohkubo, S. Kanazawa and J. S. Chang: Czech. J. Phys, Suppl. D, **52** (2002) D413